

Motion behavior of non-metallic particles under high frequency magnetic field

ZHANG Zhong-tao(张忠涛)^{1,2}, GUO Qing-tao(郭庆涛)³, YU Feng-yun(于风云)²,
LI Jie(李捷)^{1,2}, ZHANG Jian(张剑)^{1,2}, LI Ting-ju(李廷举)^{1,2}

1. State Key Laboratory of Materials Modification by Laser, Ion and Electron Beams, Dalian 116024, China;
2. School of Materials Science and Engineering, Dalian University of Technology, Dalian 116024, China;
3. Center for Computer-Aided Solidification Processing, Yonsei University Metallurgical System Engineering, Seoul 120749, Korea

Received 14 July 2008; accepted 24 October 2008

Abstract: Non-metallic particles, especially alumina, are the main inclusions in aluminum and its alloys. Numerical simulation and the corresponding experiments were carried out to study the motion behavior of alumina particles in commercial pure aluminum under high frequency magnetic field. At the meantime, multi-pipe experiment was also done to discuss the prospect of continuous elimination of non-metallic particles under high frequency magnetic field. It is shown that: 1) results of numerical simulation are in good agreement with the experimental results, which certifies the rationality of the simulation model; 2) when the intensity of high frequency magnetic field is 0.06 T, the 30 μm alumina particles in melt inner could migrate to the edge and be removed within 2 s; 3) multi-pipe elimination of alumina particles under high frequency magnetic field is also effective and has a good prospect in industrial application.

Key words: non-metallic particles; high frequency magnetic field; motion behavior; multi-pipe elimination

1 Introduction

With the rapid growth of aerospace, automobile and electronic industry, high-quality aluminum alloy is eagerly needed. The non-metallic inclusions can reduce strength, fatigue resistance and plasticity of aluminum alloy. Many efforts have been taken to separate the non-metallic inclusions from aluminum melt, such as gravity sedimentation, flotation, flux refinement and filtration[1–3]. Electromagnetic field offers very clean processes, and it is an emerging technology for the production of high-quality aluminum alloys to meet the demand both for high melt cleanliness level and for the ecological processing of materials[4]. SHU et al[5] and ZHANG et al[6] utilized alternating magnetic field to eliminate inclusions from melt, and the results showed that alternating magnetic field is effective in separating inclusion particles. The study of TAKAHASHI[7] showed that high frequency magnetic field is also effective in separating inclusions. XU et al[8] studied the continuous separation of non-metallic particles under stationary magnetic field and DC current. The particles more than 15 μm can be continuously removed. High

magnetic field was also used in the separation of particles, while it is still hard to be widely used[9]. In our earlier study[10], primary silicon in hypereutectic aluminum-silicon alloy was chosen to simulate non-metallic particle and study the motion behavior of non-metallic particles under high frequency magnetic field. In this work, the motion behavior of alumina, the main inclusion in aluminum alloys, is carried out under high frequency magnetic field. At the meantime, in order to explore the further application of this method, multi-pipe separation experiment is also carried out to explore the industrial prospect of the above method.

2 Principle

LEENOV and KOLIN[11] advanced the theory that nonconductive inclusions could be removed by electromagnetic extrusion force in conductive fluid according to their difference in conductivity. When the molten metal containing non-metallic particles is put into electromagnetic field, nonconductive inclusions could move in the direction against the electromagnetic force to the edge of tube. After that, they will be captured by the tube wall and eliminated. The forces on a particle

under electromagnetic field is shown in Fig.1[12].

Based on the analysis of KOLIN[13], the electromagnetic extrusion force can be described as follows:

$$F_p = -\frac{3}{4} \left(\frac{\sigma_f - \sigma_p}{2\sigma_f + \sigma_p} \right) \cdot \frac{\pi d_p^3}{6} \cdot f, \quad f = J \times B \quad (1)$$

where F_p is the electromagnetic extrusion force; f is the electromagnetic force; σ_f and σ_p are the conductivities of fluid and particles, respectively; d_p is the diameter of inclusion particle. When σ_p is very small compared with σ_f , it is seemed to be zero, and Eq.(1) predigests to Eq.(2):

$$F_p = -\frac{3}{4} \frac{\pi d_p^3}{6} f \quad (2)$$

where the minus represents that F_p is against f .

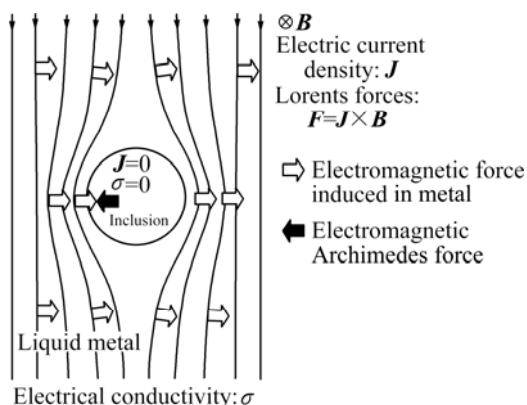


Fig.1 Principle of elimination of inclusions by use of electromagnetic field

The maximum velocity of the particle (v_{max}) in melt under electromagnetic extrusion force can be described as:

$$v_{max} = -\frac{d_p^2}{24\mu} \cdot f \quad (3)$$

where μ is the movement viscosity of melt.

According to the theory above, some models can be built to describe the motion behavior of particles under electromagnetic field. In building the models, some approximate parameters are used, and the applicability of the models needs to be tested.

In our research, high frequency magnetic field is chosen owing to its high efficiency and the schematic view of the principle is shown in Fig.2. According to Faraday’s law of electromagnetic induction, alternating magnetic field can generate induction electric field. When high magnetic field is applied, it can generate induced current in the edge of the ceramic tube owing to skin effect. The magnetic field and induced electric current interact with each other and an electromagnetic

force is generated to push the liquid metal inward. As the conductivity of non-metallic inclusions is much less than that of liquid metal, an electromagnetic extrusion force is generated and acts on the particles and pushes them outward opposite to the direction of electromagnetic force. Under electromagnetic extrusion force, the inclusions inside the melt can migrate to outer very fast.

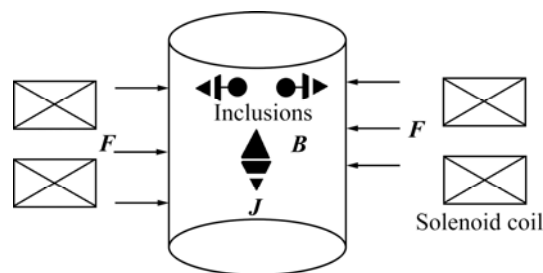


Fig.2 Effect on motion behavior of inclusion particles under high frequency magnetic field

3 Simulation and experiments

3.1 Numerical simulation

The mathematical model was built to study the motion behavior of non-metallic particles under high frequency magnetic field with the changes of the following parameters: the magnetic intensity, action time, diameter of inclusion and the diameter of the pipe. The model was described in detail in Ref.[14], and the corresponding experiments were carried out to study the motion behavior of the alumina particles in aluminum melt. By comparing the results between numerical simulation and experiments, the applicability of the model could be identified.

3.2 Experiments

3.2.1 Experimental apparatus

Fig.3 presents the schematic view of the experimental apparatus, which consists of an IGBT magnetic generator, a SG2-5-12 electric resistance furnace and solenoid coil. IGBT medium-frequency counter has a maximum power of 20 kW and the frequency of 20 kHz. The 9-turn solenoid loop is made up of copper with 10 mm in diameter. The inner diameter of the solenoid loop is 66 mm and its length is 140 mm. The magnetic field density is measured by 7030 Gauss/Tesla meter produced by Bell Laboratory.

3.2.2 Experimental procedure

Commercial pure 99.7% aluminum was used in this experiment. The alumina particles in this work were obtained by adding silica sand to aluminum melt according to the reaction under high temperature[15–16]. The alumina was mainly in the diameter from about 30 μm to 100 μm . The mixed melt was made in an electric resistance furnace. When the temperature came to 720

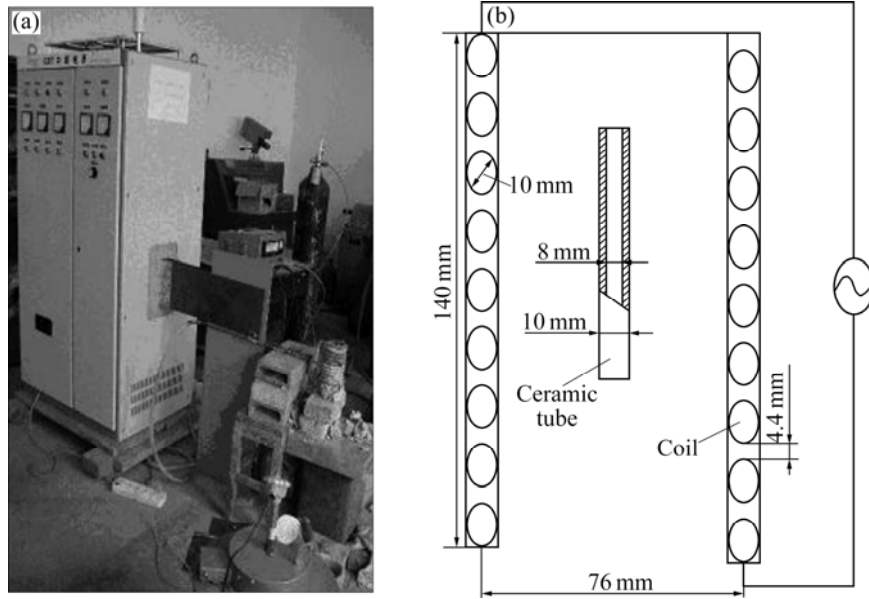


Fig.3 Apparatus of experimental (a) and schematic of coil (b)

°C, the melt was held for 30 min, and then the melt was poured into ceramic tube with diameter of 10 mm. The applied magnetic field intensities were 0.04 T and 0.06 T and the corresponding action times were 1, 2, 3, 4, 5, 10 s and 1, 2, 5 s. Multi-pipe elimination experiment was also carried out with seven pipes together and the diameters(*D*) of the pipes were all 10 mm. The applied magnetic intensity was 0.04 T and the action time was 10 s. The schematic view of the relative position of the pipes is shown in Fig.4. The samples were cooled in air, cut transversely and mechanically ground for further test.

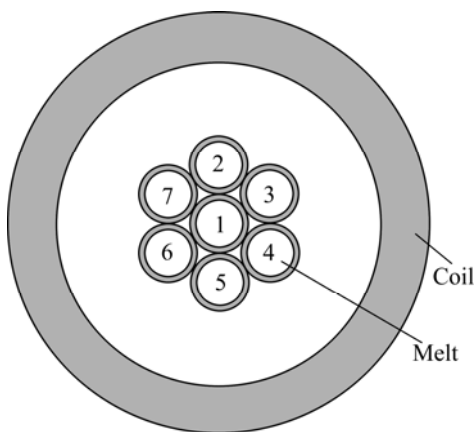


Fig.4 Schematic of electromagnetic elimination with multi-tubule

3.2.3 Analysis method

EPMA was used to test the composition of the particles. Optical microscope (MEF4) and SEM (JSM-5600LV) were used to observe and measure the macro- and micro-distribution of alumina particles, respectively.

4 Results and discussion

4.1 Simulation results and discussion

Fig.5 shows the relationship between action time and position of the non-metallic particles with different magnetic intensities. With the increase of magnetic intensity, the non-metallic particle can reach the edge much faster, owing to the increase of extrusion force on the particle. When it is 0.04 T, the particles with the diameter of 30 μm reach the edge within 12 s. While in the experimental conditions, it only needs 5 s.

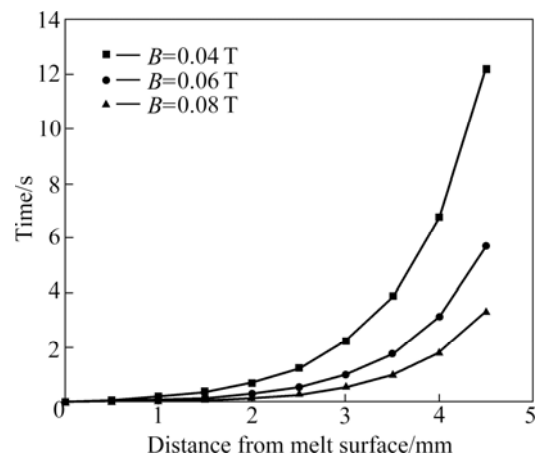


Fig.5 Simulation result of relationship between action time and position of non-metallic particles with different magnetic induction intensity (*D*=10 mm, *d_p*=30 μm)

The relationship between action time and position of the various diameter particles in the molten aluminum is shown in Fig.6. When *B*₀=0.06 T, it only needs 1 s for

the particles more than 30 μm to reach the edge, which is very fast and efficient. While to those smaller particles, it takes a long time for them to transport to the edge, which may be caused by the turbulence generated by magnetic induced flow[10]. In experiments, it needs about 2 s under 0.06 T magnetic field for the alumina particles to migrate to the edge. The simulation result is in accordance with the experiment, although there is a slim

error between them.

4.2 Experimental results and discussion

In order to determine whether the particle added into the melt is alumina or not, EPMA test is used. Fig.7 shows the EPMA image of the non-metallic particles of the sample. From the EPMA analysis, the particle is identified to be alumina particle.

The macro-morphologies of samples with $B_0=0.04$ T are shown in Fig.8. In the original sample, the alumina inclusion particles distribute evenly all over the sample

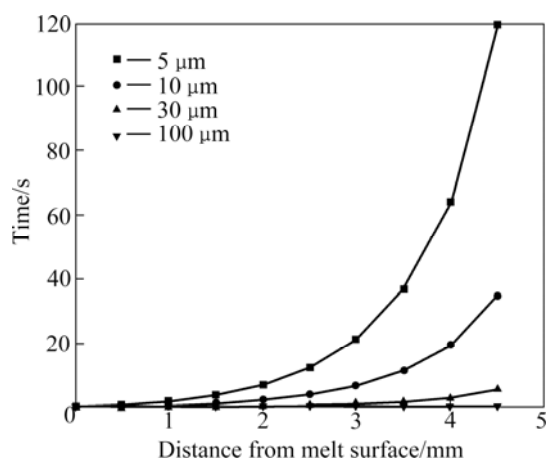


Fig.6 Simulation result of relationship between action time and position of various diameter particles ($D=10$ mm, $d_p=30$ μm , $B=0.06$ T)

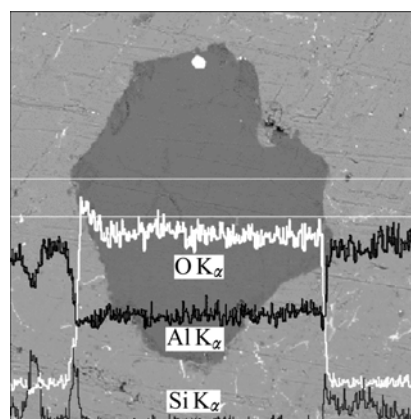


Fig.7 EPMA photo of particle in aluminum melt

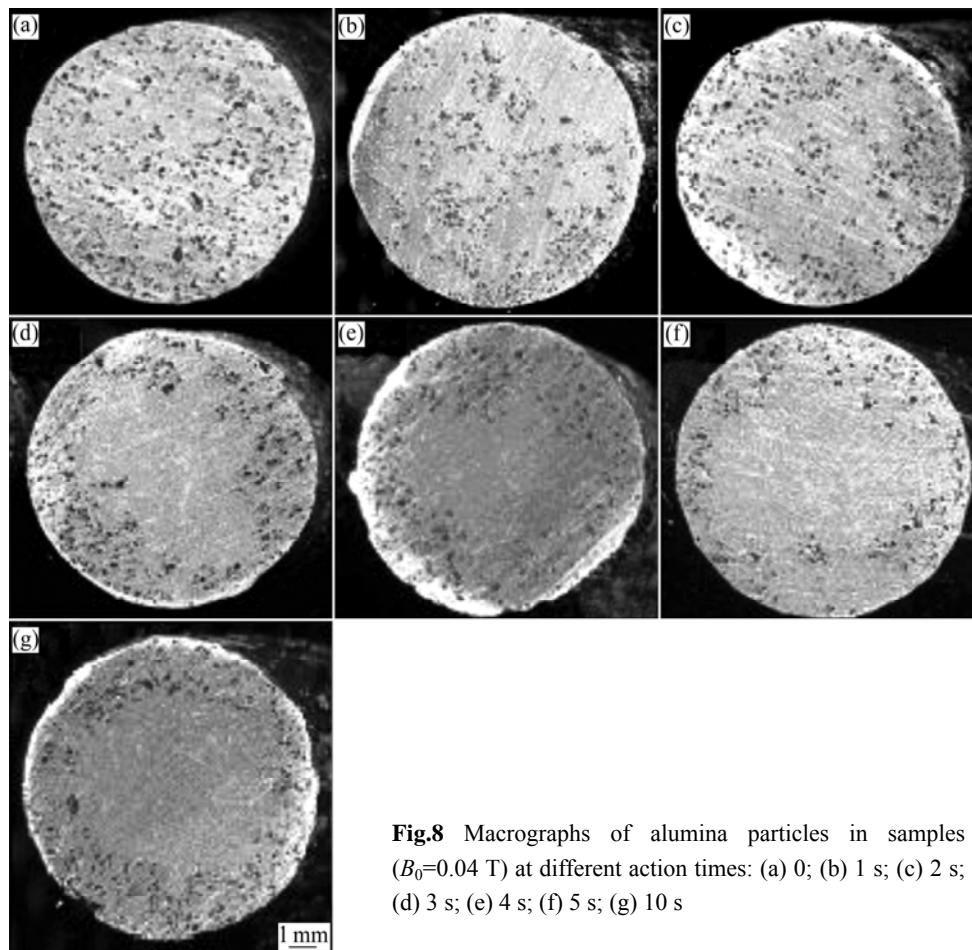


Fig.8 Macrographs of alumina particles in samples ($B_0=0.04$ T) at different action times: (a) 0; (b) 1 s; (c) 2 s; (d) 3 s; (e) 4 s; (f) 5 s; (g) 10 s

surface (Fig.8(a)). In Figs.8(b) and (c), the alumina aggregation layer forms on the edge of the tube, while there are still many big particles in the inner. There are nearly no particles visible in the inner after the action time is more than 3 s, as shown in Figs.8(d)–(g).

The SEM micrograph of the samples with the action time of 3 s is shown in Fig.9. From Fig.9(a), alumina particles in the inner are most in the diameter of about 10 μm , and a little particles with the diameter of 20 μm also exist there. While on the edge of the sample, many particles with larger diameter of 30–100 μm gather there. With the increase of particle size, the migration velocity increases much, and the bigger particles can migrate much faster than the smaller ones. In addition, smaller particles are easily affected by some unstable factors such as turbulence. They can easily go back to the melt because the driven flow is caused by the turbulence. In order to eliminate those small particles with the size of 10 μm , some methods like increasing coil turns and electric current should be adopted[17].

Fig.10 shows the macrographs of samples under $B_0=0.06$ T. When the action time is only 1 s, the effect is obvious with only several particles in the inner (Fig.10(a)). When the separation time is 5 s, there are no particles bigger than 30 μm visible by naked eye inside of the sample.

Fig.11 shows the SEM micrographs of the samples under $B_0=0.06$ T with separation time 5 s. The particles all migrate outside under electromagnetic extrusion force. As shown in Fig.11(a), no particles more than 30 μm could be seen in the inner. The particles with the

maximum size of 100 μm all aggregate to the outer layer of the samples, as seen in Fig.11(b). With the increase of the magnetic intensity, the external force on a particle is larger, and so is the velocity of the particle. When they reach the edge, they are captured by the internal wall of the ceramic tube. At the meantime, they can agglomerate with each other to form larger particles, which can facilitate the motion velocity and elimination efficiency.

The results of multi-pipe elimination of alumina particles are shown in Fig.12. Most of the particles in pipes migrate outside under electromagnetic extrusion force of high frequency magnetic field for 10 s. In multi-pipe experiments, when several tubules exist simultaneously, they can affect each other and the outer melt can have a shielding effect on the melt in the inner, which can bring some negative effects on the inner. Owing to the interaction among pipes, the elimination effect is not as good as the single pipe experiment. While in our experiments, through adjusting the experimental parameters like action time, magnetic intensity and distance between the tubules, satisfied elimination results can be obtained. The multi-pipe experiment brings a good prospect for the wide use of high frequency magnetic field on the separation of non-metallic particles. This might bring a new method to produce high-quality aluminum alloys.

The numerical simulation and experimental results are in good agreement to a great extent, although there are some errors between them. The possible reasons are: 1) The effect of shapes of inclusion particles is ignored; 2) The viscosity is continuously changed in actual

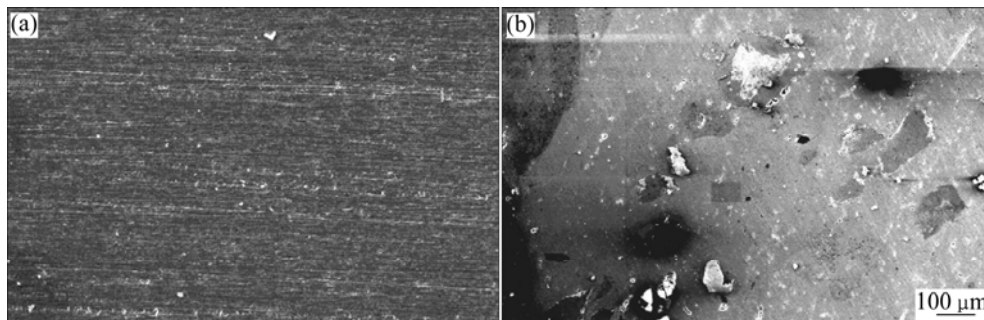


Fig.9 SEM micrographs of sample with action time of 3 s ($B_0=0.04$ T): (a) Inner of sample; (b) Edge of sample

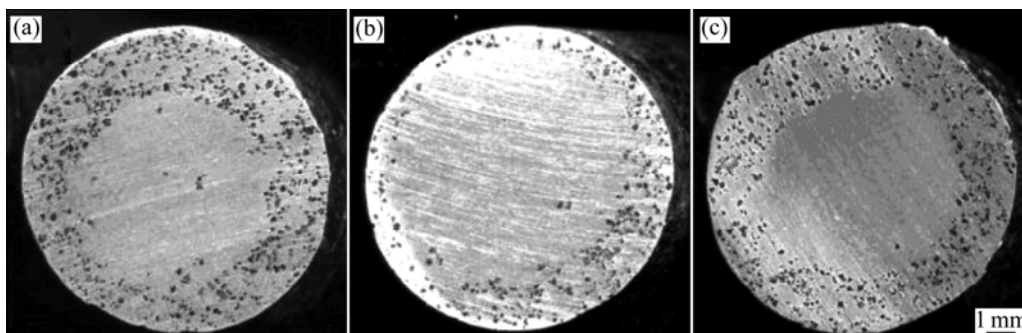


Fig.10 Macrostructures of distribution of alumina particles in sample ($B_0=0.06$ T) at different times: (a) 1 s; (b) 2 s; (c) 5 s

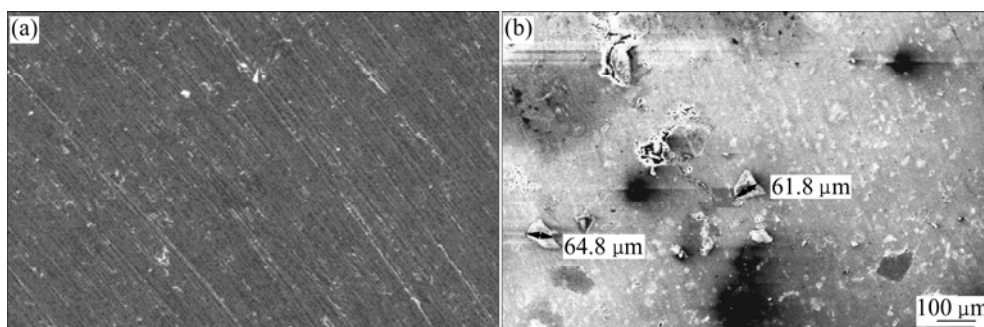


Fig.11 SEM micrographs of sample with separation time of 5 s ($B_0=0.06$ T): (a) Inner of sample; (b) Edge of sample

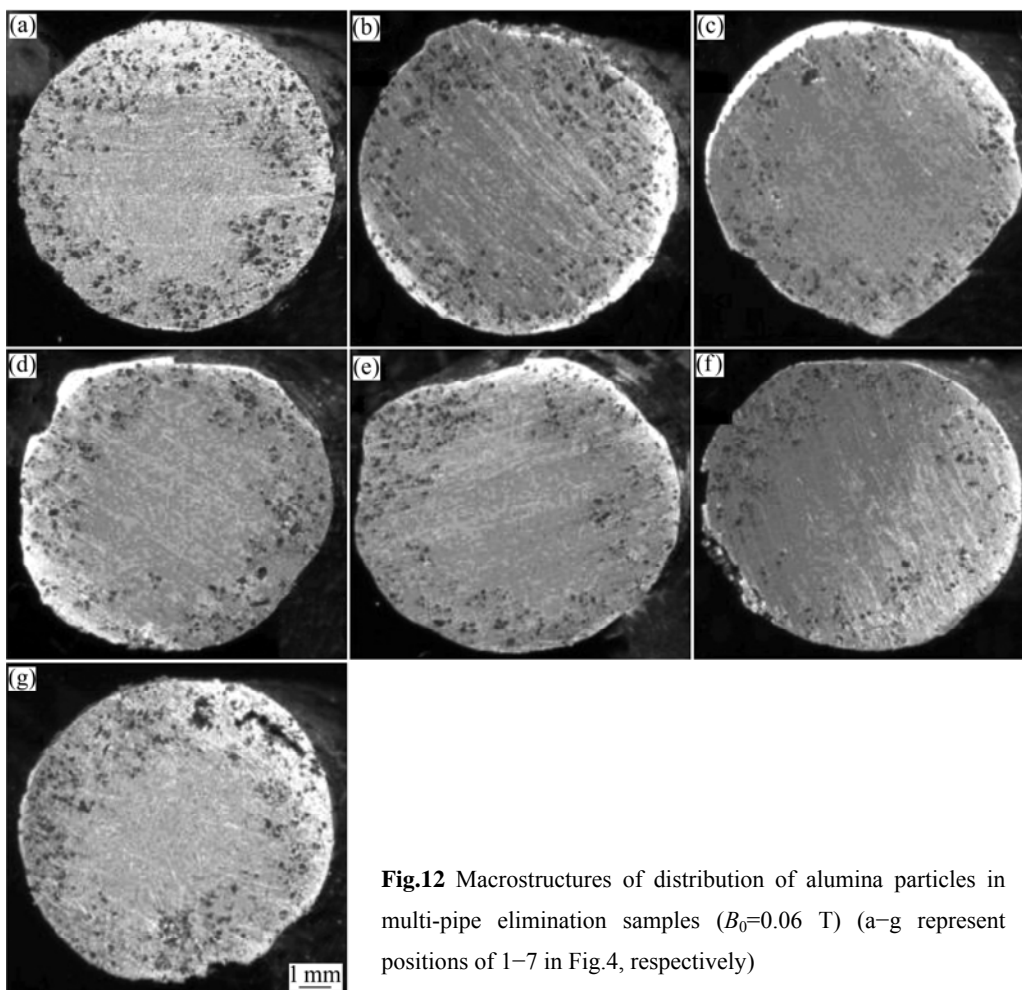


Fig.12 Macrostructures of distribution of alumina particles in multi-pipe elimination samples ($B_0=0.06$ T) (a–g represent positions of 1–7 in Fig.4, respectively)

conditions, while in the simulation conditions it is considered to be constant; 3) There is turbulence in the course of particles motion, which is ignored in theoretical analysis.

5 Conclusions

1) The results of numerical simulation are in good agreement with the experimental results, which validates the rationality of the simulation model.

2) When the intensity of high frequency magnetic

field is 0.06 T, the 30 μm alumina particles in melt inner could migrate to the edge and be removed within 2 s.

3) The multi-pipe separation of alumina particles under high frequency magnetic field is also effective and has a good prospect in industrial application.

References

- [1] GALVIN K P, CALLEN A, ZHOU J, DOROODCHI E. Performance of the reflux classifier for gravity separation at full scale [J]. Minerals Engineering, 2005, 18(1): 9–24.
- [2] TRAHAR W J, WARREN L J. The flotability of very fine particles—

- A review [J]. *International Journal of Mineral Processing*, 1976, 3(2): 103–131.
- [3] CAO Xin-jin. A new analysis of pressure filtration curves for liquid aluminum alloys [J]. *Scripta Materialia*, 2005, 52(9): 839–842.
- [4] SHU Da, LI Tiao-xiao, SUN Bao-de, WANG Jun, ZHOU Yao-he. Study of electromagnetic separation of nonmetallic inclusions from aluminum melt [J]. *Metallurgical and Materials Transactions A*, 1999, 30(11): 2979–2988.
- [5] SHU Da, SUN Bao-de, LI Ke, LI Tian-xiao, XU Zhen-ming, ZHOU Yao-he. Continuous separation of non-metallic inclusions from aluminum melt using alternating magnetic field [J]. *Materials Letters*, 2002, 55(5): 322–326.
- [6] ZHANG Bang-wen, REN Zhong-ming, WU Jia-xiang. Continuous electromagnetic separation of inclusion from aluminum melt using alternating current [J]. *Trans Nonferrous Met Soc China*, 2006, 16(1): 33–38.
- [7] TANIGUCHI K. Electromagnetic separation of nonmetallic inclusion from liquid metal by imposition of high frequency magnetic field [J]. *ISIJ Int*, 2003, 43: 820–827.
- [8] XU Zhen-ming, LI Tiao-xiao, ZHOU Yao-he. Continuous removal of nonmetallic inclusions from aluminum melts by means of stationary electromagnetic field and DC current [J]. *Metallurgical and Materials Transactions A*, 2007, 38(5): 1104–1110.
- [9] MA Yan-wei, XIAO Li-ye, YAN Lu-guang. Application of high magnetic fields in advanced materials [J]. *Chinese Science Bulletin*, 2006, 51: 2944–2950.
- [10] GUO Qing-tao, LI Ting-ju, WANG Tong-min, JIN Jun-ze, CAO Zhi-qiang, ZHANG Qi. Effect of turbulent flow on electromagnetic elimination with high frequency magnetic field [J]. *Trans Nonferrous Met Soc China*, 2006, 16(5): 1141–1147.
- [11] LEENOV D, KOLIN A. Theory of electromagnetophoresis (I): Magnetohydrodynamic forces experienced by spherical and symmetrically oriented cylindrical particles [J]. *J Chem Phys*, 1954, 22(4): 683–688.
- [12] ASAI S. Recent development and prospect of electromagnetic processing of materials [J]. *Science and Technology of Advanced Materials*, 2000, 1(4): 191–200.
- [13] KOLIN A. An electromagneto kinetics phenomenon involving migration of neutral particles [J]. *Science*, 1953, 117(6): 134–137.
- [14] GUO Qing-tao, JIN Jun-ze, LI Ting-ju, WANG Tong-min, ZHANG Qi, CAO Zhi-qiang. Mathematical model of electromagnetic elimination in tubule with high frequency magnetic field [J]. *Trans Nonferrous Met Soc China*, 2006, 16(1): 47–51.
- [15] RAJAN T P D, PILLAI R M, PAI B C. Interfacial reactions in aluminosilicate short fiber-reinforced aluminum matrix composites [J]. *Metallurgical and Materials Transactions A*, 2002, 33: 2755–2761.
- [16] TSUNEKAWA Y, SUZUKI H, GENMA Y. Application of ultrasonic vibration to in situ MMC process by electromagnetic melt stirring [J]. *Materials and Design*, 2001, 22(6): 467–472.
- [17] LI Ming-jun, ZHAI Xiu-jing, SUN Zhong-qi, YAO Guang-chun. Numerical simulation of particulate inclusion movement during electromagnetic separation from molten aluminium [J]. *Journal of Northeastern University: Natural Science*, 2001, 22(2): 143–145.

(Edited by YANG Hua)